European Journal of Mechanics A/Solids ••• (••••) •••–•••

Contents lists available at ScienceDirect

European Journal of Mechanics A/Solids

www.elsevier.com/locate/ejmsol

Overspeed burst of elastoviscoplastic rotating disks – Part I: Analytical and numerical stability analyses

M. Mazière [a,*], J. Besson [a], S. Forest [a], B. Tanguy [a], H. Chalons [b], F. Vogel [b]

[a] MINES ParisTech, MAT - Centre des Matériaux, CNRS UMR 7633, BP 87, 91003 Evry Cedex, France
[b] Turbomeca, F-64511 Bordes, France

ARTICLE INFO

Article history:
Received 7 June 2007
Accepted 18 July 2008

Keywords:
Stability
Bifurcation
Non-linear behaviour
Rotating disks
Spin-softening
Computational mechanics
Nickel based superalloys

ABSTRACT

Burst of rotating disks in case of overspeed is investigated. The certification of turbo-engines requires to demonstrate the integrity of disks at higher rotation speeds than the maximum rotation speed reachable in service. The determination of the burst speed by analysis can help to reduce the number of tests required for the certification. This prediction can be established by non-linear stability analyses of finite element simulations. Non-linearities originate from (i) the material behaviour described by elastoviscoplastic constitutive equations, (ii) geometric changes accounted for by the finite strain formulation. In this work, loss of uniqueness and loss of stability criteria from [Hill, R., 1958. A general theory of uniqueness and stability in elastic-plastic solids. J. Mech. Phys. Solids 6, 236–249] are applied. The loss of stability criterion is restricted to the case of rotating disks and compared to several simple widely used material based failure criteria. 3D simulations of rotating metal disks are performed for a given elastoviscoplastic behaviour and the stability criteria are evaluated. The sensitivity of disk stability to material parameters, such as yield criterion, hardening and viscosity is evaluated in the case of a nickel based superalloy.

1. Introduction

In a turbo-engine, components are submitted to severe conditions in term of temperature gradient and centrifugal loading. Despite high operating rotation rates, designs are such that global deformation remains reversible. However, overspeed events may occur. In order to prevent any effect of overspeed on flight safety, Airworthiness Requirements (CS-E or FAR,...) impose to protect disks from burst by overspeed securities (electronic and/or mechanical protection,...) and to demonstrate the integrity of the engine rotors at significantly higher rates than the operating rotation speed. Therefore, turbo-engine manufacturers have to conduct disk burst analyses and disk integrity tests. In order to validate the disk burst analyses, burst tests of experimental rotating disks are carried out. Burst of experimental rotating disks may occur in one the following modes: (i) in a "rim peel" burst, a portion of the outer diameter comes off while the hub section remains intact, (ii) in a "hoop mode" burst, the entire disk disintegrates along radial planes in two or more parts. Research concerning rotating disks bursts has been focused on: (I) the prediction from a limit plastic analysis of the maximum suitable value of the angular velocity in case of overspeed, (II) the prediction of the number of burst fragments, (III) the prediction of unexpected bursts due to fatigue crack propagation, which is not related to an overspeed issue.

(I): Among the earliest works concerning response of disks to centrifugal loads, the elastic analytical studies carried out in Love (1927), Timoshenko and Goodier (1934), Roark and Young (1982) document on the stress and strain fields. These results have been used in Laszlo (1948), Percy et al. (1974) to suggest that burst occurs when the mean hoop stress on a disk section becomes equal to the nominal tensile strength of the material, determined from an uniaxial tensile stress. This criterion shows good correlation with experimental results for rotating rings, but for solid or bored disks Tvergaard wonders if this criterion gives a precise estimate of the maximum angular velocity (Tvergaard, 1978), and Manavi recommends the use of a burst factor between both aforementioned stresses (Manavi, 2006). Moreover, Tvergaard carries out a comparative review of several burst criteria, using an original numerical method, for ductile bored disks of uniform thickness. Nowadays, the average hoop stress criterion is still used, but the evaluation of the burst factor highly depends on disk geometries. It will be shown in Section 3.4 to be inappropriate for a non-axisymmetric disk. Another empirical criterion, appropriate for finite element simulations associates burst with the step of calculation when a critical value of the cumulated plastic strain is reached for the first time at any integration point. This local criterion referred to as the "critical strain criterion", strongly depends on the material behaviour, especially on the shape of the hardening curve. The

* Corresponding author. Tel.: +33 1 60 76 30 45.
E-mail address: maziere@mat.ensmp.fr (M. Mazière).

0997-7538/$ – see front matter
doi:10.1016/j.euromechsol.2008.07.008

validity of this criterion for ductile rotating disks will also be discussed in Section 3.4.

(II): Assuming a crack in a plane delimited by axial and radial directions, the post-critical state of disks has been studied by Kohl and Dhondt (1993), Dhondt (1994), Bert and Paul (1995), Dhondt and Kohl (1999). The number of burst fragments, and the translational kinetic energies of containment, are predicted, depending on the ratio of outside to inside radius of the disk. These studies are useful in the case of small turbines like auxiliary power units, where the certification requires that such fragments should be contained at a normal rotation speed.

(III): Fatigue fracture surfaces have been observed in Park et al. (2002), Bhaumik et al. (2002) on burst disks. This case differs from the overspeed situation, as burst is caused by a fatigue crack unstable propagation at normal operating speed. Turbine disks have basically three critical regions where fatigue cracks can develop: the fir-tree rim region, the assembly holes, and the hub region. Many investigations have been performed, using finite element simulations, to evaluate the number of cycles required for a crack to grow from an initial size to a final critical size, or to locate critical areas of the structure, corresponding to high radial, hoop or von Mises stress values. Meguid in (Meguid et al., 2000) shows that maximum stresses are underestimated in fir-tree region with 2D finite element analyses, and recommend the use of a 3D model. In the same region, Claudio investigated the influence of the initial crack position (Claudio et al., 2004), and Witek locates accurately the critical areas close to the fir-tree (Witek, 2006). The same kind of analysis is conducted in Zhuang (2000) on assembly hole region. Newman outlined the influence of different load sequences in any region (Newman, 1996). Finally, a probabilistic fracture analyses is performed in Liu et al. (2005), Walz and Riesch-Oppermann (2006) to take into account the non-uniformity of the material. The sensitivity of the number of cycles to failure with respect to the number and size of defects, and material properties such as yield and fracture stress, are evaluated.

The present study focuses on computing the regulation reserve factor of the rotation rate for an overspeed turbo-engine disk. Generalised plasticity is assumed to be responsible for burst, as in (I). A numerical stability analysis for overloaded disks is performed using elastoplastic or elastoviscoplastic constitutive laws at large strain. In order to reproduce the experimental testing procedure, the angular velocity is prescribed in simulations. The case where the angular momentum is prescribed is not discussed in this article. In the former case, burst of disks occurs when the limit rotation rate is reached while increasing the angular velocity. The average hoop stress and the critical strain criteria (cf. (I)) are shown to be inaccurate to predict this burst speed for any geometry. A multiaxial stability criterion for burst, coinciding with the maximum of the load displacement curve is presented, based on the modified global second order work (MSOW). The first two criteria do not take into account spin-softening effect, which represents the increase of centrifugal load with radial deformation. This effect is also neglected in most studies about rotating disk, which are performed within a small deformation formulation (Witek, 2006; Manavi, 2006). Non-uniform material properties or disks geometries are also not usually considered, except in Tvergaard (1978) where imperfections in the thickness of disks of uniform section are taken into account. Finally, time-dependent effects such as material viscosity and inertial terms have never been accounted for in simulations of overspeed burst of rotating disks to our knowledge. In this paper, an important and new feature of the analysis is the study of the influence of plasticity model and material parameters on burst rotation rate. The choice of the yield function will be shown to be of the utmost importance on speed burst prediction. Accounting for material rate-dependency and dynamic effects is also a new feature in the analysis of rotating disks.

This study begins with a brief description of the finite strain constitutive elastoplastic equations (Besson et al., 2001). The incremental formulation of a mechanical problem is then presented in order to introduce Hill's stability and uniqueness criteria (Hill, 1958, 1959; Petryk, 1993; Tvergaard, 1993; Nguyen, 2000a). Three different burst criteria for rotating disks are then presented and compared. Hill's global stability criterion is first specialised to the case of a rotating disk. A term corresponding to the spin-softening effect is evidenced. In Section 3.2 describing the empirical "critical strain" criterion, some simple analytical examples with homogeneous solutions are treated in order to compare it with the "global stability" criterion introduced previously. The results in terms of plastic strain at the onset of instability, are compared in the case of simple tension, simple shear, and rotating ring, for two different nickel-base superalloys. The "average hoop stress" criterion is also described. Finally, these three criteria are evaluated on finite element simulations of different rotating geometries. In Section 4, time-independent finite element simulations are performed on an actual industrial power turbine disk. The mechanical response beyond the critical angular velocity, and the limit angular velocity associated with the loss of stability given by Hill's criterion, are obtained using an arc-length control method (Riks, 1979; Crisfield et al., 1997; Jirasek and Bazant, 2002; Germain et al., 2007). An important issue, not systematically studied in literature, is the influence of the material model and parameters. Simulations are carried out with different yield criteria, and hardening laws. In the last part, time-dependent effects are accounted for in simulations of rotating disks. The effect of viscosity in addition to elastoplastic material law is first evaluated. Then dynamic simulations are performed including inertial terms in the mechanical formulation. In both cases, since the arc-length control method cannot be used anymore, the loss of stability is analysed based on Hill's stability criteria.

2. Stability and uniqueness

2.1. Problem formulation

The finite strain formulation for isotropic non-linear material behaver adopted in this work is based on the use of a local objective frame as proposed in Sidoroff and Dogui (2001), Besson et al. (2001), Bertram (2005). Observer invariant stress and strain rate measures $\underset{\sim}{\boldsymbol{s}}$ and $\underset{\sim}{\dot{\boldsymbol{e}}}$ are defined by transport of the Cauchy stress $\underset{\sim}{\boldsymbol{T}}$ and strain rate $\underset{\sim}{\boldsymbol{D}}$ into the corotational frame characterised by the rotation $\underset{\sim}{\boldsymbol{Q}}(\underline{\boldsymbol{x}}, t)$. This change of frame takes place at each material point:

$$\begin{cases} \underset{\sim}{\boldsymbol{s}} = \underset{\sim}{\boldsymbol{Q}} \cdot \underset{\sim}{\boldsymbol{T}} \cdot \underset{\sim}{\boldsymbol{Q}}^T, \\ \underset{\sim}{\dot{\boldsymbol{e}}} = \underset{\sim}{\boldsymbol{Q}} \cdot \underset{\sim}{\boldsymbol{D}} \cdot \underset{\sim}{\boldsymbol{Q}}^T, \\ \underset{\sim}{\boldsymbol{Q}} \text{ such that } \underset{\sim}{\dot{\boldsymbol{Q}}}^T \cdot \underset{\sim}{\boldsymbol{Q}} = \underset{\sim}{\boldsymbol{\Omega}} \text{ (corotational)}. \end{cases} \tag{1}$$

The strain rate $\underset{\sim}{\dot{\boldsymbol{e}}}$ is then split into elastic and viscoplastic contributions, the evolution of the latter being given by the yield function $f(\underset{\sim}{\boldsymbol{s}}, R)$. Formally, this method makes it possible to keep the same evolution equations for internal variables as in the small strain framework. A yield criterion f, associated to an equivalent stress measure $s_{\text{eq}}(\underset{\sim}{\boldsymbol{s}})$, and an isotropic hardening law $R(p)$ are retained for the elastoplastic model:

$$\begin{cases} \underset{\sim}{\dot{\boldsymbol{e}}} = \underset{\sim}{\dot{\boldsymbol{e}}}^e + \underset{\sim}{\dot{\boldsymbol{e}}}^p, \\ f(\underset{\sim}{\boldsymbol{s}}, R) = s_{\text{eq}}(\underset{\sim}{\boldsymbol{s}}) - R(p), \\ \underset{\sim}{\dot{\boldsymbol{e}}}^p = \dot{p} \frac{\partial f}{\partial \underset{\sim}{\boldsymbol{s}}}, \quad \dot{p} \geqslant 0, \\ \underset{\sim}{\boldsymbol{s}} = 2\mu \underset{\sim}{\boldsymbol{e}}^e + \lambda \operatorname{tr}(\underset{\sim}{\boldsymbol{e}}^e) \underset{\sim}{\boldsymbol{1}}. \end{cases} \tag{2}$$

Please cite this article in press as: M. Mazière et al., Overspeed burst of elastoviscoplastic rotating disks – Part I: Analytical and numerical stability analyses, European Journal of Mechanics A/Solids (2008), doi:10.1016/j.euromechsol.2008.07.008

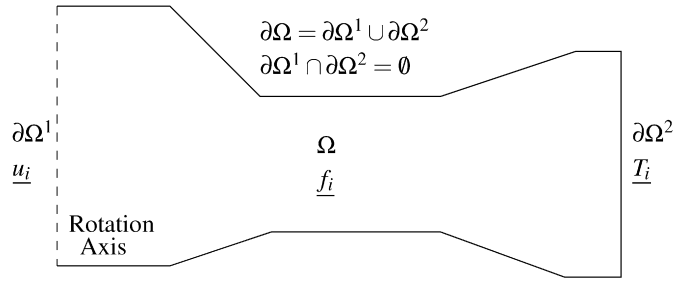

Fig. 1. General mechanical problem of a rotating disk.

In the plastic case, $\dot{p}$ is obtained using the consistency condition. In the viscoplastic case, a viscoplastic flow rule $g(f)$ is added to compute the cumulative viscoplastic strain increment $\dot{p}$, where g is an invertible monotonic function:

$$\dot{p} = g(f). \tag{3}$$

A solid Ω (initially Ω_0) is submitted to kinematical constraints on the part $\partial\Omega^1$ (initially $\partial\Omega_0^1$) of its boundary, to surface loads $\underline{\boldsymbol{T_i}}$ (expressed as $\underline{\boldsymbol{T_i}}_0$ on $\partial\Omega_0^2$) on the part $\partial\Omega^2$ (initially $\partial\Omega_0^2$), and to body forces $\underline{\boldsymbol{f_i}}$ (expressed as $\underline{\boldsymbol{f_i}}_0$ on Ω_0), as shown in Fig. 1.

The governing field equations of the problem are:

$$\begin{cases} \text{Material behavior;} \\ \text{Equilibrium: } \operatorname{div}_X \underset{\sim}{\boldsymbol{S}} + \rho_0 \underline{\boldsymbol{f_i}} = \underline{\boldsymbol{0}} \quad \text{on } \Omega_0; \\ \text{Boundary conditions: } \underline{\boldsymbol{u}} = \underline{\boldsymbol{u_i}} \quad \text{on } \partial\Omega_0^1, \ \underset{\sim}{\boldsymbol{S}} \cdot \underline{\boldsymbol{N}} = \underline{\boldsymbol{T_i}} \quad \text{on } \partial\Omega_0^2 \end{cases} \tag{4}$$

where $\underset{\sim}{\boldsymbol{S}}$ denotes the first Piola–Kirchhoff stress tensor. The two last equations can be combined in the weak formulation called the principle of virtual power:

$$\underbrace{\int_{\Omega_0} \underset{\sim}{\boldsymbol{S}} : \underset{\sim}{\dot{\boldsymbol{F}}}^* \, dv_0}_{P_{\text{INT}}} = \underbrace{\int_{\Omega_0} \rho_0 \underline{\boldsymbol{f_i}} \cdot \underline{\boldsymbol{V}}^* \, dv_0 + \int_{\partial\Omega_0^2} \underline{\boldsymbol{T_i}} \cdot \underline{\boldsymbol{V}}^* \, ds_0}_{P_{\text{EXT}}},$$

$$\forall \underline{\boldsymbol{V}}^* \text{ such that } \underline{\boldsymbol{V}}^* = \underline{\boldsymbol{0}} \text{ on } \partial\Omega_0^1 \quad \text{with } \underset{\sim}{\dot{\boldsymbol{F}}}^* = \frac{\partial \underline{\boldsymbol{V}}^*}{\partial \underline{\boldsymbol{X}}}. \tag{5}$$

It is useful to define an incremental formulation of the mechanical problem by time derivation of (4). The global form of this incremental formulation is called the principle of virtual second order work (Nguyen, 2000a)

$$\operatorname{div}_X \underset{\sim}{\dot{\boldsymbol{S}}} + \rho_0 \underline{\boldsymbol{f_i}} = \underline{\boldsymbol{0}} \quad \text{on } \Omega_0, \tag{6}$$

$$\underbrace{\int_{\Omega_0} \underset{\sim}{\dot{\boldsymbol{S}}} : \underset{\sim}{\dot{\boldsymbol{F}}}^* \, dv_0}_{P^{(2)}_{\text{INT}}} = \underbrace{\int_{\Omega_0} \rho_0 \underline{\boldsymbol{f_i}} \cdot \underline{\boldsymbol{V}}^* \, dv_0 + \int_{\partial\Omega_0^2} \underline{\boldsymbol{T_i}} \cdot \underline{\boldsymbol{V}}^* \, ds_0}_{P^{(2)}_{\text{EXT}}},$$

$$\forall \underline{\boldsymbol{V}}^* \text{ such that } \underline{\boldsymbol{V}}^* = \underline{\boldsymbol{0}} \text{ on } \partial\Omega_0^1. \tag{7}$$

2.2. Hill uniqueness and stability conditions

Two fundamental criteria for loss of uniqueness of the solution of the boundary value problem, and loss of stability of an equilibrium, respectively, can be deduced from the previous incremental formulation of the finite strain mechanical problem. They have been derived by Hill (1958, 1959) under restricted conditions. They have been extended gradually to more general cases (Nguyen, 2000a). A sufficient condition for uniqueness is established by considering two different solutions of the problem.

Uniqueness is ensured if $\forall(\underline{\boldsymbol{V_1}}, \underline{\boldsymbol{V_2}})$ *kinematically admissible* ($\underline{\boldsymbol{V_1}} = \underline{\boldsymbol{V_2}} = \underline{\boldsymbol{V_i}}$ *on* $\partial\Omega_0^1$),

$$\int_{\Omega_0} \Delta \underset{\sim}{\dot{\boldsymbol{S}}} : \Delta \underset{\sim}{\dot{\boldsymbol{F}}} \, dv_0 - \left(\int_{\Omega_0} \rho_0 \Delta \underline{\boldsymbol{V}} \cdot \frac{\partial \underline{\boldsymbol{f_i}}}{\partial \underline{\boldsymbol{u}}} \cdot \Delta \underline{\boldsymbol{V}} \, dv_0 + \int_{\partial\Omega_0^2} \Delta \underline{\boldsymbol{V}} \cdot \frac{\partial \underline{\boldsymbol{T_i}}}{\partial \underline{\boldsymbol{u}}} \cdot \Delta \underline{\boldsymbol{V}} \, ds_0 \right) > 0$$

$$\text{with } \Delta(\cdot) = (\cdot)_1 - (\cdot)_2. \tag{8}$$

The second criterion is useful to detect the loss of stability of equilibrium. It can be defined as the sensitivity of the internal second order work with respect to a perturbation. This value becomes negative when equilibrium becomes unstable.

Equilibrium is stable if $\forall \underline{\boldsymbol{V}}$ *such that* $\underline{\boldsymbol{V}} = \underline{\boldsymbol{0}}$ *on* $\partial\Omega_0^1$,

$$\int_{\Omega_0} \underset{\sim}{\dot{\boldsymbol{S}}} : \underset{\sim}{\dot{\boldsymbol{F}}} \, dv_0 - \left(\int_{\Omega_0} \rho_0 \underline{\boldsymbol{V}} \cdot \frac{\partial \underline{\boldsymbol{f_i}}}{\partial \underline{\boldsymbol{u}}} \cdot \underline{\boldsymbol{V}} \, dv_0 + \int_{\partial\Omega_0^2} \underline{\boldsymbol{V}} \cdot \frac{\partial \underline{\boldsymbol{T_i}}}{\partial \underline{\boldsymbol{u}}} \cdot \underline{\boldsymbol{V}} \, ds_0 \right) > 0. \tag{9}$$

The conditions (9) and (8) look similar. It is outlined in Hill (1959), that this similarity depends on the linearity of the relation between the stress and strain rates. The $\Delta\underline{\boldsymbol{V}}$ fields admitted in (8) are exactly the admitted fields $\underline{\boldsymbol{V}}$ in (9). Indeed, both vanish on $\partial\Omega_0^1$ and are otherwise arbitrary. But the tensors $\Delta\underset{\sim}{\dot{\boldsymbol{S}}}$ and $\Delta\underset{\sim}{\dot{\boldsymbol{F}}}$ are generally not related by the same relation as $\underset{\sim}{\dot{\boldsymbol{S}}}$ and $\underset{\sim}{\dot{\boldsymbol{F}}}$. The conditions (8) and (9) are equivalent for the linear comparison solid only. A connexion exists, even for a non-linear relation, between both conditions, in the sense that (8) reduces to (9) when one field of the pair vanishes identically. Finally, relations between stability and uniqueness conditions are:

$$\begin{cases} (8) \Rightarrow (9), \\ (8) \Leftrightarrow (9) \text{ if } \underset{\sim}{\dot{\boldsymbol{S}}} = \underset{\approx}{\boldsymbol{L}} : \underset{\sim}{\dot{\boldsymbol{F}}} \\ \text{with } \underset{\approx}{\boldsymbol{L}} \text{ single-branched tangent tensor.} \end{cases} \tag{10}$$

3. Failure criteria for rotating disks

3.1. Global stability criterion (■)

Considering the mechanical problem of a rotating disk, $\underline{\boldsymbol{V_i}} = \underline{\boldsymbol{0}}$ and the $\underline{\boldsymbol{V}}$ fields admissible in (9) are kinematically admissible for (8). In some mechanical problems, external loads $\underline{\boldsymbol{f_i}}$ and $\underline{\boldsymbol{T_i}}$ do not depend on displacements in the structure. Then the second term in Eqs. (8) and (9) vanishes. In contrast, the centrifugal load at a point M of the structure depends on the current radius r at this point. Because this radius increases during the loading sequence, the load also increases even if the angular velocity remains constant. This effect is called spin-softening. It makes the second term of the criteria non-zero, and promotes instability. This term has been evaluated in order to rewrite more specifically the stability criterion for rotating disks:

Equilibrium is stable if $\forall \underline{\boldsymbol{V}}$ *kinematically admissible*,

$$\text{MSOW} = \int_{\Omega_0} \left(\underset{\sim}{\dot{\boldsymbol{S}}} : \underset{\sim}{\dot{\boldsymbol{F}}} - \rho_0 \| \underline{\boldsymbol{V}} \times \underline{\boldsymbol{\omega}} \|^2 \right) dv_0 > 0 \tag{11}$$

where $\underline{\boldsymbol{\omega}}$ is the vector of angular velocity, $\times$ is the vector product, and $\| \cdot \|$ denotes the Euclidean norm of the vector.

If one can find $\underline{\boldsymbol{V}}$ such that this global modified second order work (MSOW) becomes negative, stability is lost.

The first term in Eq. (11) is referred to as the Second Order Work (SOW). The whole expression, taking into account the spin softening term, is called the Modified Second Order work (MSOW). Criterion (11) detects the limit point of the rotation rate versus displacement equilibrium curve, by looking at the sign of modified second order work as given by the finite element solution.

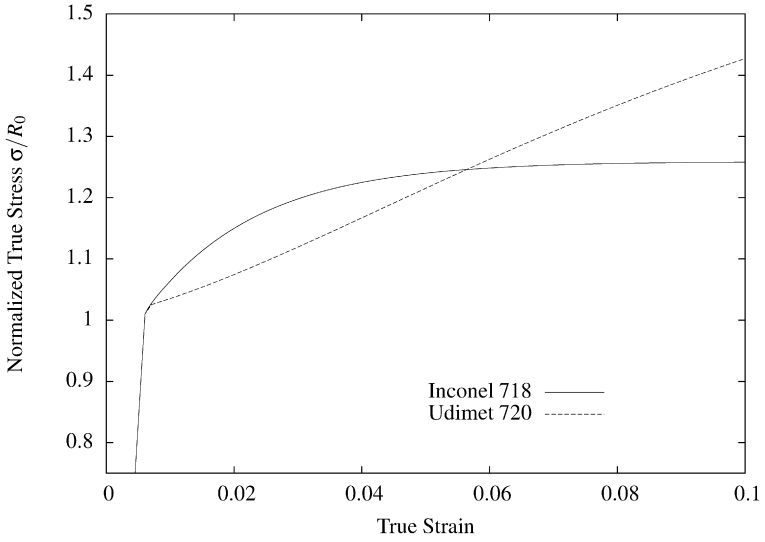

Fig. 2. Example of tensile behaviour of Inconel 718 and Udimet 720. R_0 denotes the yield stress.

When the velocity field produced by this solution, $\underline{\boldsymbol{V}}_{\text{FEM}}$, makes condition (11) fail, the limit point is reached, and the solution becomes unstable and non-unique. The search for instabilities is not performed for all kinematically admissible velocity fields, but only for the current finite element solution. It must be noted that the maximal rotation rate is reached when the MSOW vanishes, while the maximal average load is reached when the SOW vanishes. This method is not essential in the case of time-independent finite element simulations, since the maximum of the equilibrium curve can also be detected easily if they are performed with an accurately formulated arc-length control method. Indeed, the load parameter in the arc-length control method can be associated either with the rotation rate or with the external load. In the first case, the maximum of the load parameter is then associated with the maximum of the rotation rate and consequently with the loss of stability of the structure. However, in the case of time-dependent simulations, the stability criterion (11) will be useful to detect the loss of stability of disks and consequently their limit rotation rate.

3.2. Critical strain criterion (▲)

In this section, the relevance of the empirical "critical strain" burst criterion is investigated. This criterion sometimes used in practical applications associates burst with the first step of calculation where a given critical cumulated plastic strain is reached at an integration point. The critical cumulated plastic strain is provided by the uniaxial tensile curve, and corresponds to the point where the external load is maximum (limit point). The stability criterion previously defined is applied here to three simple mechanical problems (simple tension, simple shear and rotating ring) solved for a purely plastic material behaviour. The analytical problems are solved with a plane stress formulation at large deformations. The stress and strain fields are homogeneous in the structure, at least before instabilities occur. Actually, instability can take place as soon as geometrical softening becomes larger than material hardening. Two different Nickel based superalloys are chosen for the computation.

First, a plate is submitted to a tensile test. The critical cumulated plastic strain p^{LIM} for which instability occurs is given by the solution of the following equation:

$$p^{\text{LIM}} \text{ is such as } \frac{\partial R}{\partial p}\left(p^{\text{LIM}}\right) = R\left(p^{\text{LIM}}\right). \tag{12}$$

This criterion is the one formulated in Considère (1885). Then, a plate is submitted to a simple shear test controlled by applied displacements. The critical cumulated von Mises plastic strain p^{LIM} is provided by the solution of the following equation:

$$p^{\text{LIM}} \text{ solution of } \frac{\partial R}{\partial p}\left(p^{\text{LIM}}\right) = 2\sqrt{3}\tan\left(2\sqrt{3}p^{\text{LIM}}\right)R\left(p^{\text{LIM}}\right). \tag{13}$$

Finally, the stability of a rotating ring is evaluated. The critical cumulated plastic strain p^{LIM} for which instability occurs is given by the solution of the following equation:

$$p^{\text{LIM}} \text{ is such as } \frac{\partial R}{\partial p}\left(p^{\text{LIM}}\right) = 2R\left(p^{\text{LIM}}\right). \tag{14}$$

These analytical solutions are applied to two different materials. Both are nickel-based superalloys and their Beauvoir can be represented by non-linear hardening laws without viscosity effect represented in Fig. 2. For both superalloys $R(p)$ is of the following form:

$$R(p) = R_0 + Q_1\left(1 - \exp(-b_1 p)\right) + Q_2\left(1 - \exp(-b_2 p)\right) \tag{15}$$

where R_0 is the initial yield stress. The parameters for both materials are given in Table 1.

The critical plastic strains p^{LIM} are given in Table 2 for both materials, and for the three different tests (simple tension, simple shear, and rotating ring).

One can observe significant differences between the critical values calculated for both materials. Differences between tension and shear arise from the form of the two hardening curves. In the case of Inconel 718, the critical strain for simple tension is lower than

Table 1
Non-linear isotropic hardening parameters for two Nickel based superalloys (Inconel 718 and Udimet 720) at room temperature

Parameters	E (GPa)	R_0 (MPa)	Q_1 (MPa)	b_1	Q_2 (MPa)	b_2
Inconel 718	200	1217	1614	58	−1380	58
Udimet 720	200	1227	2118	15.1	−1280	22.1

Table 2
Critical plastic strains for three tests (simple tension, simple shear, and rotating ring), and both Nickel based superalloys (Inconel 718 and Udimet 720)

p^{LIM}	Tension	Shear	Rotating ring
Inconel 718	0.042	0.05	0.027
Udimet 720	0.21	0.15	0.11

Please cite this article in press as: M. Mazière et al., Overspeed burst of elastoviscoplastic rotating disks – Part I: Analytical and numerical stability analyses, European Journal of Mechanics A/Solids (2008), doi:10.1016/j.euromechsol.2008.07.008

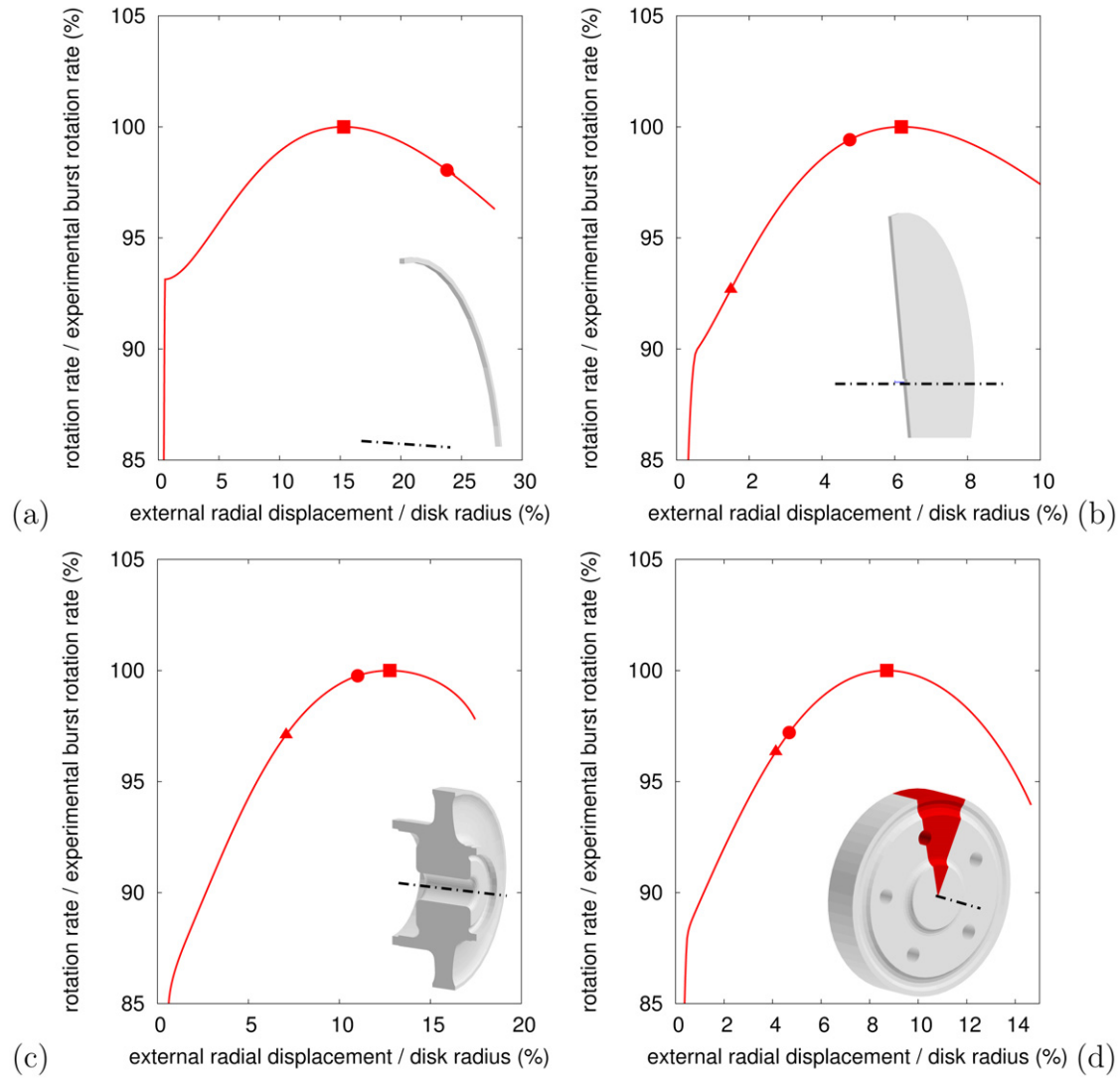

Fig. 3. Comparison of the three burst criteria on the equilibrium curve for (a) a rotating ring, (b) an axisymmetric rotating disk with rectangular section, (c) an axisymmetric turbine disk (d) a non-axisymmetric turbine disk. The "critical strain" criterion is marked with ▲, the "average hoop stress" criterion with ●, the "global stability" criterion with ■. ▲ and ● coincide on figure (a).

for simple shear. The use of uniaxial strain criteria would probably be conservative for many problems. In contrast, in the case of Udimet 720, the critical strain for simple shear is lower than for simple tension. Differences between tension and rotating ring are due to the spin-softening effect. For example, the critical strain in tension for a rotating ring (0.21 for Udimet 720) is associated with the maximum hoop load, while the ring critical strain (0.11 for Udimet 720) is associated with the maximum of rotation rate. Because of the spin-softening effect, both maxima do not coincide. Then, in the first case (tension) the critical hoop load is detected, while in the second one (rotating ring) the limit rotation rate corresponding to the loss of stability of the structure given by Hill's criterion is detected.

3.3. *Average hoop stress criterion* (●)

This semi-empirical criterion has been proposed in Robinson (1944): a disk will burst when the average hoop nominal stress equals the tensile strength of the material. The hoop nominal stress is provided by the corresponding component of the first Piola–Kirchhoff stress tensor. This criterion is found to be slightly conservative (Percy et al., 1974) for rotating disks with rectangular section. Two main approximations are made using this criterion. First, the spin-softening effect is not considered and the limit average hoop load is detected instead of the limit rotation rate. Secondly, the multiaxiality of stress tensor in rotating disks is not taken into account and the limit load is then underestimated. Since both approximations are acting in opposite ways, this criterion provides usually an accurate estimation of the limit rotation rate, at least for axisymmetric disks.

3.4. *Comparison of burst criteria on several disks geometries*

The three aforementioned criteria have been tested on four different geometries (cf. Fig. 3), using finite element simulations. The "global stability" criterion obviously allows to determine the maximum rotation rate for each simulation. The two other criteria are fulfilled either before or after this point and consequently they are underestimating or overestimating the limit rotation rate. In the case of a rotating ring they gives the maximum load. Otherwise, the non-uniformity of deformations and the stress multiaxiality makes these criteria more or less accurate. They are particularly far from the limit rotation rate in the case of a non-axisymmetric turbine disk. The latter geometry is used for the sensitivity analysis presented in the following section.

Please cite this article in press as: M. Mazière et al., Overspeed burst of elastoviscoplastic rotating disks – Part I: Analytical and numerical stability analyses, European Journal of Mechanics A/Solids (2008), doi:10.1016/j.euromechsol.2008.07.008

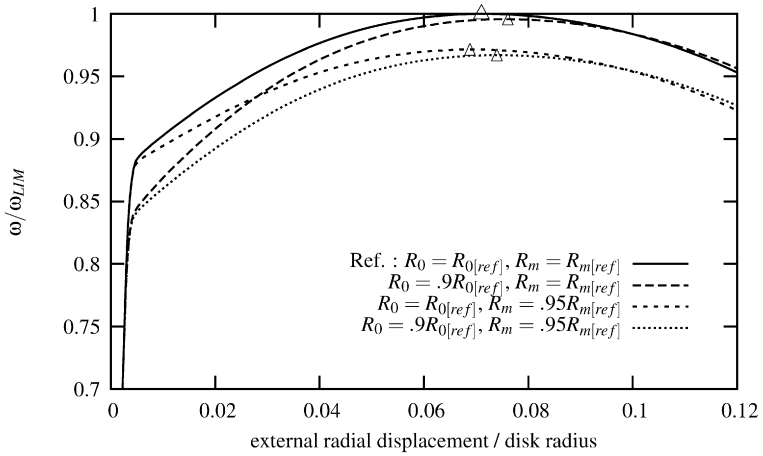

Fig. 4. Influence of hardening law on the equilibrium curve; comparison for different R_0 and R_m. [ref] means that parameters values for Udimet 720 are given in Table 1.

4. Time-independent finite element simulations of overspeed test

Simulations presented in Section 3.4 are carried out on a power turbine disk with the Zset finite element program (Besson and Foerch, 1997). Due to the presence of assembly holes, one tenth of the disk, the red area in Fig. 3(d), has been meshed with height nodes linear elements (for colors see the web version of the article). The selective integration method (Hughes, 1980) is used with a finite strain formulation and the elastoplastic law for Udimet 720. The computation is controlled by the applied centrifugal load. An arc-length method is used (Riks, 1979), in order to avoid numerical divergence close to the limit point and to overcome it. Blades are taken into account in the computation by the addition of mass elements on the external side of the disk.

The influence of material parameters such as yield criterion, and hardening law, on the equilibrium curve are investigated in the following sections. Each parameter is modified and the equilibrium curve representing the normalised angular velocity versus the normalised radial displacement on rim of disks is compared to the reference curve. The instability point corresponding to the limit angular velocity ω_{LIM} is estimated from the global criterion (11). It is marked with a $\triangle$ on the reference curve.

4.1. Influence of the hardening law

Devy et al. (1990) have shown that during forming process of disks, quenching rate can vary by a ratio of 10 between core and skin of the disk, implying a 10% difference in the hardening level. However, after final heat treatments this difference is no more significant. But the material properties have to be particularly well identified at least up to the ultimate stress. The influence of the hardening law is presented in Fig. 4. The reference curve corresponding to the elastoplastic law for Udimet 720 used previously is compared to three different hardening laws: one with a 10% reduction of R_0, one with a 5% reduction of R_m, and one with both reductions. R_m denotes there the ultimate true tensile stress i.e. $R_m = R_0 + Q_1 + Q_2$ (see (15)). The yield stress R_0 has no real influence on the limit angular velocity, which is however very sensitive to ultimate stress R_m.

4.2. Influence of yield criterion

The plastic behaviour is described by a yield surface that evolves during deformation. The yield function specifies the shape of this surface, while the hardening law provides its evolution. Two criteria representing this surface have been proposed by Tresca (1864) and Mises (1913). Both are characterised by different expressions of the equivalent stress s_{eq} in the yield equations (2). The yield stress can be chosen such that all criteria coincide in tension. Then they strongly differ for simple shear. For the latter stress state, the ratio between equivalent stresses for the same strain is maximal and equal to $\sqrt{3}/2$ or 13.5%. It is shown in Love (1927), Timoshenko and Goodier (1934), Roark and Young (1982) that a rotating disk is mostly submitted to biaxial stresses where the tangential stress is around twice the radial one, like for a plane strain test. These differences between the results obtained by simulations with both criteria (Tresca and von Mises) are shown in Fig. 5. The two yield criteria have been identified such that the tensile curve is the same. Considering the limit angular velocity ω^{LIM}, the difference is as high as 7%. This clearly shows the importance of selecting the best suited yield function for the considered material.

5. Time-dependent finite element simulations of overspeed test

Time plays a role in finite element simulations in two cases: (i) when the material behaviour is rate-dependent, (ii) when a dynamic simulation is performed evaluating inertial terms in the equilibrium equation. In both cases, the arc-length control method used in Section 4 cannot be used in a straight forward manner to determine the loss of stability of structures. Hill's stability criterion becomes essential to estimate the limit rotation rate of rotating disks.

5.1. Influence of viscosity

Rate-dependency is introduced by a function $g(f)$ between the plastic strain rate $\dot{p}$ and the yield surface f as in Eq. (3). The following viscous flow rule is adopted:

$$\dot{p} = g(f) = \dot{\varepsilon}_0 \sinh\left(\frac{f}{\sigma_0}\right). \tag{16}$$

The rate sensitivity increases when σ_0 increases. The influence of this parameter for three different value of σ_0 and for the reference hardening parameters are given in Fig. 6. A conventional load control method was then used. The ultimate angular velocity ω_{LIM} is approximated from the criterion (11), when the MSOW tends to zero (see Fig. 7). Actually, the MSOW never becomes negative and the stability is consequently never lost. But this latter becomes closer and closer to zero while the rotation rate remains almost constant. An accurate estimation of the limit rotation rate may then be extrapolated as shown on Fig. 7. This critical angular velocity ω_{LIM} increases when the rate sensitivity increases. The

Please cite this article in press as: M. Mazière et al., Overspeed burst of elastoviscoplastic rotating disks – Part I: Analytical and numerical stability analyses, European Journal of Mechanics A/Solids (2008), doi:10.1016/j.euromechsol.2008.07.008

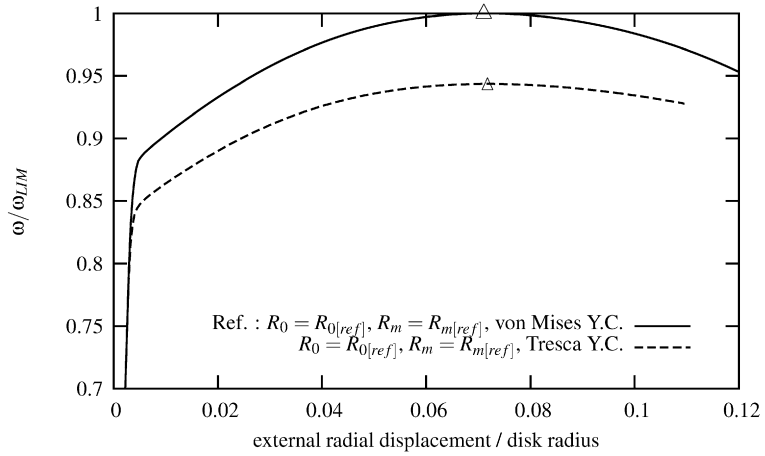

Fig. 5. Influence of yield criterion on the equilibrium curve; comparison between von Mises and Tresca criteria for the reference material parameters for Udimet 720.

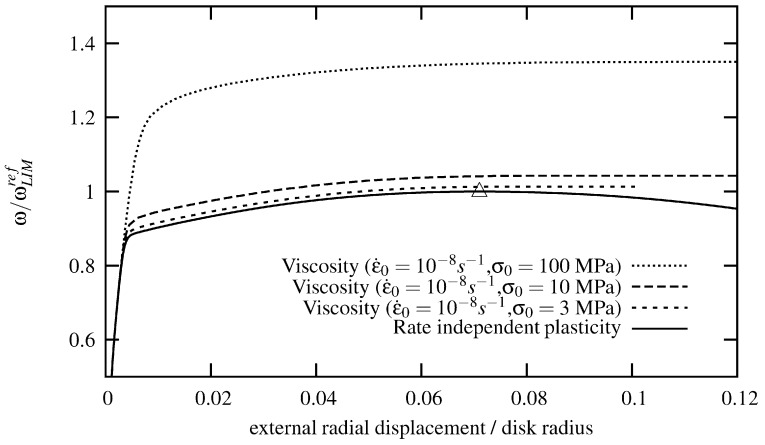

Fig. 6. Influence of viscosity on the equilibrium curve. $\omega_{\mathrm{LIM}}^{\mathrm{ref}}$ is the limit rotation rate for the purely plastic reference behaver.

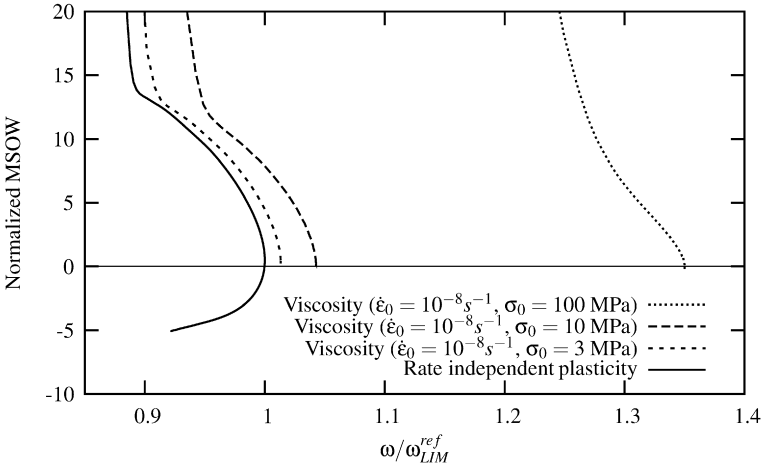

Fig. 7. Modified second order work (MSOW) versus relative rotation rate for simulations of Fig. 6. The MSOW is normalised with respect to the spin-softening term: $\int_{\Omega_0}(\rho_0\|\underline{\boldsymbol{V}}\times\underline{\boldsymbol{\omega}}\|^2)\,dv_0$. When the MSOW is negative or equal to zero, stability is lost.

rate sensitivity of the material makes rotating disks more stable in terms of angular velocity.

5.2. Influence of inertial terms

In most finite element simulations of rotating disks, the inertial terms of the equilibrium equation are neglected as done in the boundary value problem (4), assuming that deformation rates are usually low enough during most of the loading path. However, when the rotation rate reaches its limit value, these rates may become significant enough. Like in Section 5.1, the arc-length control method is not applicable directly, even for time-independent material behaviour, because of the time-dependency of the equilibrium equation. The equilibrium curve of a dynamic simulation for a rate independent material behaviour is compared with the corresponding static one on Fig. 8. Even if the Hill's stability criterion

Please cite this article in press as: M. Mazière et al., Overspeed burst of elastoviscoplastic rotating disks – Part I: Analytical and numerical stability analyses, European Journal of Mechanics A/Solids (2008), doi:10.1016/j.euromechsol.2008.07.008

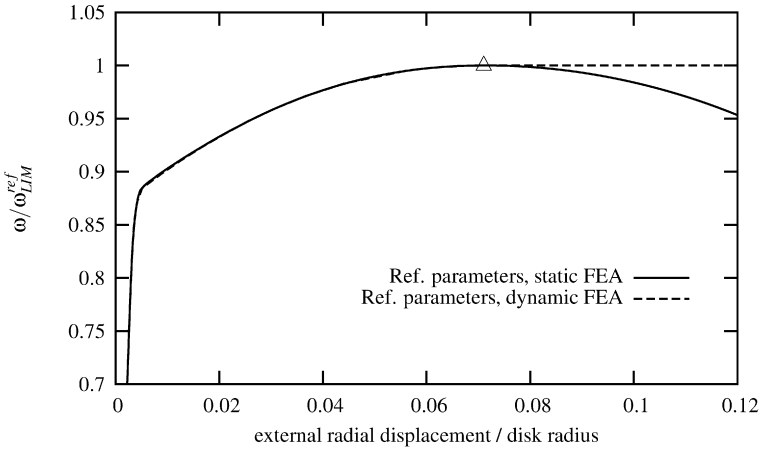

Fig. 8. Influence of inertial terms on the equilibrium curve.

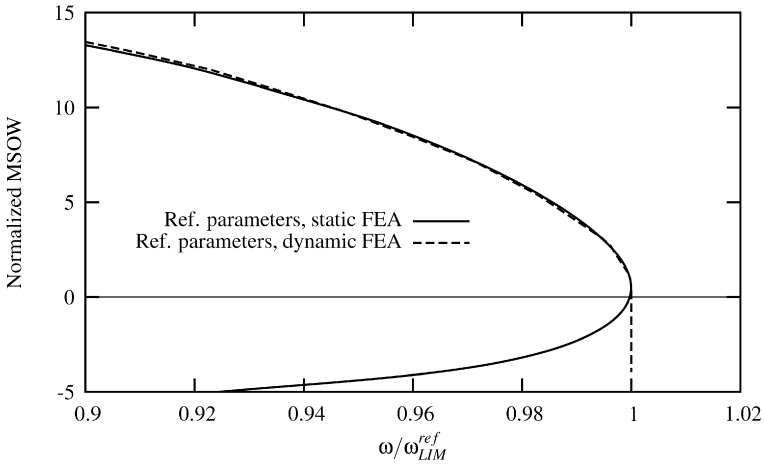

Fig. 9. Modified second order work (MSOW) versus relative rotation rate for simulations of Fig. 8. The MSOW is normalised with respect to the spin-softening term: $\int_{\Omega_0}(\rho_0\|\underline{\boldsymbol{V}}\times\underline{\boldsymbol{\omega}}\|^2)\,dv_0$. When the MSOW is negative or equal to zero, stability is lost.

is established from static equilibrium equations, it can be accepted as a dynamic stability criterion (Nguyen, 2000b). The limit rotation rate is then estimated using the sign change of the modified second order work (cf. Fig. 9). This latter is found nearly equal to the quasi-static simulation one.

6. Conclusions

Burst of rotating disks in case of overspeed was assumed to be due to generalises plasticity. To detect the corresponding critical rotation rate, Hill's stability criterion was applied to the case of centrifugal loading. This criterion was shown to be more accurate than other existing engineering criteria to predict the limit rotation rate of any rotating disk for any material behaver. It was applied in two different ways depending on the type of material behaviour and finite element simulation.

(I) In case of time-independent material behaviours and simulations, Hill's stability criterion was implicitly applied using an arc-length control method. The role of the material parameter and plasticity model was then studied. The critical angular velocity is mainly controlled by the ultimate stress (R_m) whereas the yield stress (R_0) plays a limited role. The Tresca yield criterion leads to a lower critical velocity (about 7%) than the von Mises criterion for the same tensile behaviour. The dependence of the critical rotation rate on the material constitutive equations shows than an accurate characterisation of the material behaviour is required when a precise evaluation (i.e. $\pm 10\%$) of ω_{LIM} is needed.

(II) In case of time-dependent material behaviours or simulations, Hill's stability criterion was explicitly applied from an a posteriori estimate of the modified second order work (MSOW). The material viscosity leads to an increase of the limit rotation rate as compared to a time-independent material showing an equivalent hardening law. Accounting for inertial terms in finite element simulation does not modify the limit rotation rate, at least if the overspeed simulation time scale remains in agreement with the experimental one. The last finite element simulation presented in this work provides the most complete and realistic description of an overspeed burst test for which the angular velocity is prescribed.

Acknowledgements

This work has been carried within the common project DDV leaded by ONERA (French Aeronautics and Space Research Center) and funded by the DGA (French Ministry of Defense) which is gratefully acknowledged.

References

Bert, C., Paul, T., 1995. Failure analysis of rotating disks. Int. J. Solids Structures 32, 1307–1318.

Bertram, A., 2005. Elasticity and Plasticity of Large Deformations. Springer.

Besson, J., Cailletaud, G., Chaboche, J.-L., Forest, S., 2001. Mécanique non-linéaire des matériaux. Hermes.

Besson, J., Foerch, R., 1997. Large scale object–oriented finite element code design. Comp. Meth. Appl. Mech. Engrg. 142, 165–187.

Bhaumik, S., et al., 2002. Failure of turbine rotor blisk of an aircraft engine. Engrg. Failure Anal. 9, 287–301.

Claudio, R., et al., 2004. Fatigue life prediction and failure analysis of a gaz turbine disc using the finite element method. Fatigue and Fract. Engrg. Mater. Struct. 27, 849–860.

Considère, A., 1885. L'emploi du fer et de l'acier dans les constructions. In : Annales des ponts et chaussées, ENSPC, pp. 574–775.

Crisfield, M., Jelenic, G., Mi, Y., Zong, H., Fan, Z., 1997. Some aspects of the non-linear finite element method. Finite Element and Design 27, 19–40.

Devy, F., Benallal, A., Boucherit, A., Marquis, D., Mosser, P., 1990. Modélisation de la trempe l'huile de disques de turboréacteurs en superalliage base nickel. Revue Française de Mécanique 2, 143–157.

Dhondt, G., 1994. Failure analysis of aircraft engine disks II. Int. J. Solids Structures 31, 1949–1965.

Dhondt, G., Kohl, M., 1999. The effect of the geometry and the load level on the dynamic failure of rotating disks. Int. J. Solids Structures 36, 789–812.

Germain, N., Besson, J., Feyel, F., Gosselet, P., 2007. High-performance parallel simulation of structure degradation using non-local damage models. Int. J. Numer. Meth. Engrg. 71, 253–276.

Hill, R., 1958. A general theory of uniqueness and stability in elastic-plastic solids. J. Mech. Phys. Solids 6, 236–249.

Hill, R., 1959. Some basic principles in the mechanics of solids without a natural time. J. Mech. Phys. Solids 7, 209–225.

Hughes, T., 1980. Generalization of selective integration procedures to anisotropic and non linear media. Int. J. Numer. Meth. Engrg. 15, 1413–1418.

Jirasek, M., Bazant, Z., 2002. Inelastic Analysis of Structures. John Wiley and Sons.

Kohl, M., Dhondt, G., 1993. Failure analysis of aircraft engine disks. Int. J. Solids Structures 30, 137–149.

Laszlo, F., 1948. Rotating disks in the region of permanent deformation. Technical report, National Advisory Committee for Aeronautics.

Liu, C., Lu, Z., Xu, Y., Yue, Z., 2005. Reliability analysis for low cycle fatigue life of the aeronautical engine turbine disc structure under random environment. Math. Sci. Engrg. 395, 218–225.

Love, A., 1927. A Treatise on the Mathematical Theory of Elasticity. Dover Edition.

Manavi, B., 2006. Centrifugal rotor tri-hub burst for containment system validation. In: ASME Turbo Expo 2006: Power for Land, Sea and Air, ASME, pp. 1–9.

Meguid, S., Kanth, P., Czekanski, A., 2000. Finite element analysis of fir tree region in turbine discs. Finite Elements in Analysis and Design 35, 305–317.

Mises, R., 1913. Nachrichten von der königlichen Gelleschaft der Wissenschaften zu Gottingen, Mathematisch-physikalische Klasse. In: Mechanik der festen Korper im plastich-deformablen Zustand, pp. 582–592.

Newman, J., 1996. Application of a closure model to predict crack growth in three engine disc materials. Int. J. Fracture 80, 193–218.

Nguyen, Q., 2000a. Stabilité et mécanique non linéaire. Hermes.

Nguyen, Q., 2000b. Stability and Nonlinear Solid Mechanics. John Wiley & Sons.

Park, M., et al., 2002. Analysis of a j69-t-25 engine turbine blade fracture. Engrg. Failure Anal. 9, 593–601.

Percy, M., Ball, K., Mellor, P., 1974. An experimental study of the burst strength of rotating disks. Int. J. Mech. Sci. 16, 809–817.

Petryk, H., 1993. Theory of bifurcation and instability in time-independent plasticity. In: Bifurcation and Stability of Dissipative Systems. In: CISM Courses and Lectures. Springer-Verlag, Wien, pp. 95–152.

Riks, E., 1979. An incremental approach to the solution of snapping and buckling problems. Int. J. Solids Structures 15, 529–551.

Roark, J., Young, W., 1982. Formulas for Stress and Strain. McGraw-Hill Edition.

Robinson, E., 1944. Bursting tests of steam-turbine disk wheels. Trans. ASME 66, 373.

Sidoroff, F., Dogui, A., 2001. Some issues about anisotropic elastic-plastic models at finite strain. Int. J. Solids Structures 38, 9569–9578.

Timoshenko, S., Goodier, J., 1934. Theory of Elasticity. McGraw-Hill Edition.

Tresca, H., 1864. Mémoire sur l'écoulement des corps solides soumis de fortes pressions. C. R. Acad. Sci. Paris 59, 754.

Tvergaard, V., 1978. On the burst strength and necking behavior of rotating disks. Int. J. Mech. Sci. 20, 109–120.

Tvergaard, V., 1993. Tensile instabilities at large strains. In: Bifurcation and Stability of Dissipative Systems. In: CISM Courses and Lectures. Springer-Verlag, Wien, pp. 251–291.

Walz, G., Riesch-Oppermann, H., 2006. Probabilistic fracture mechanics assessment of flaws in turbine disks including quality assurance procedures. Structural Safety 28, 273–288.

Witek, L., 2006. Failure analysis of turbine discs of an aero engine. Engrg. Failure Anal. 13, 9–17.

Zhuang, W., 2000. Prediction of crack growth from bolt holes in a disc. Int. J. Fatigue 22, 241–250.

Please cite this article in press as: M. Mazière et al., Overspeed burst of elastoviscoplastic rotating disks – Part I: Analytical and numerical stability analyses, European Journal of Mechanics A/Solids (2008), doi:10.1016/j.euromechsol.2008.07.008